Eur. Phys. J. C (2021) 81:920
https://doi.org/10.1140/epjc/s10052-021-09522-w

THE EUROPEAN PHYSICAL JOURNAL C

Regular Article - Theoretical Physics

Gravitating Cho–Maison monopole

Khai-Ming Wong[a], **Dan Zhu, Guo-Quan Wong**

School of Physics, Universiti Sains Malaysia, 11800 USM Penang, Malaysia

Received: 25 March 2021 / Accepted: 2 August 2021 / Published online: 19 October 2021

Abstract We study numerical solutions corresponding to spherically symmetric gravitating electroweak monopole and magnetically charged black holes of the Einstein–Weinberg–Salam theory. The gravitating electroweak monopole solutions are quite identical to the gravitating monopole solution in SU(2) Einstein–Yang–Mills–Higgs theory, but with distinctive characteristics. We also found solutions representing radially excited monopole, which has no counterpart in flat space. Both of these solutions exist up to a maximal gravitational coupling before they cease to exist. Lastly we also report on magnetically charged non-Abelian black holes solutions that is closely related to the regular monopole solutions, which represents counterexample to the 'no-hair' conjecture.

1 Introduction

Since the introduction of Dirac monopole by Dirac [1,2], magnetic monopole has become a subject that attracts a lot of interest, both theoretically and experimentally. Since then the Dirac monopole has been generalized to non-Abelian monopoles, most notably Wu-Yang monopole in SU(2) Yang–Mills theory [3–5] and 't Hooft–Polyakov monopole in SU(2) Yang–Mills–Higgs (YMH) theory [6–8]. While the Dirac monopole and Wu-Yang monopole possess infinite energy due to the presence of point singularity in the solutions, the 't Hooft–Polyakov monopole possesses finite energy with no singularity found anywhere. The mass of 't Hooft–Polyakov monopole was estimated to be of order 137 $M_{\rm W}$, where $M_{\rm W}$ is the mass of intermediate vector boson.

The coupling of gravity to the SU(2) YMH theory, known as the SU(2) Einstein–Yang–Mills–Higgs (EYMH) theory has been shown to possess important solutions [9,10]. These solutions include globally regular gravitating monopole solutions, radial excitation and magnetically charged black hole solutions. For small gravitational coupling, the gravitating monopole solution emerges smoothly from flat space 't Hooft–Polyakov monopole. The (normalized) mass of gravitating monopole solution decreases with increasing gravitational coupling and the solution ceases to exist beyond a maximal value of gravitational coupling. Besides the fundamental gravitating monopole there exists radially excited monopole solution, where the gauge field function of the n-th excited monopole possess n nodes, and this is different from the gauge field function of fundamental monopole solution that decreases monotonically to zero. Having no flat space counterparts, these excited solutions are related to the globally regular Bartnik–Mckinnon solutions in SU(2) Einstein–Yang–Millls (EYM) theory [11]. There also exist magnetically charged EYMH black hole solutions which represent counterexamples to the 'no-hair' conjecture. Distinct from the embedded Reissner–Nordstrom (RN) black holes with unit magnetic charge, these black hole solutions emerge from the regular magnetic monopole solutions when a finite regular event horizon is imposed. Consequently, they have been characterized as 'black holes within magnetic monopoles'.

The SU(2) × U(1) Weinberg-Salam theory has been shown to possess important topological magnetic monopole solution, known as the electroweak monopole or simply Cho–Maison monopole [12,13]. As a hybrid between Dirac monopole and 't Hooft–Polyakov monopole, the Cho–Maison monopole describes a real monopole dressed by the physical W-boson and Higgs field. Although the Cho–Maison monopole has a singularity at the origin which makes the energy divergent, it has been shown there are ways to regularize the energy and estimating the mass at 4–10 TeV [14–16]. Recently, there is also reports on a more natural way to regularize the energy, suggesting that the new BPS bound for the Cho–Maison monopole may not be smaller than 2.98 TeV, more probably 3.75 TeV [17]. As mentioned also in Ref. [17], the discovery of electroweak monopole should be interpreted as an important topological test of the standard model. This makes the experimental detection of electroweak

[a] e-mail: kmwong@usm.my (corresponding author)

monopole an urgent issue after the discovery of Higgs boson. For this reason experimental detectors around the globe are actively searching for magnetic monopole [18–24].

Recently gravitationally coupled electroweak mono-pole solutions in Einstein–Weinberg–Salam (EWS) theory has also been reported by Cho et al. [25]. Their results confirm the existence of globally regular gravitating electroweak monopole solution, before changes to the magnetically charged black hole as the Higgs vacuum value approaches to the Planck scale.

In this paper, we study in more detail the gravitating electroweak monopole in EWS theory, and report additional radially excited electroweak monopole solution, as well as the corresponding 'black hole within electroweak monopole' solutions of the EWS theory. Our results therefore confirm that all solutions found in the SU(2) EYMH theory [9,10] have their corresponding counterpart in the EWS theory, but with distinctive functional behaviour. From the physical point of view, these solutions are very important as Weinberg-Salam theory itself is a realistic theory.

More recently, there is also report on spherically symmetric magnetic and dyonic black holes with magnetic charge $Q = 2$ in the Standard Model and general relativity [26]. The results is a magnetically charged black hole with mass below 9.3×10^{35} GeV that possesses a 'hairy' cloud of electroweak gauge and Higgs fields outside the event horizon with $1/M_{\rm W}$ in size. Considering also the dyonic part, it is shown that an extremal magnetic black hole has a hair mass of 3.6 TeV, while an extremal dyonic black hole has an additional mass of $q^2 \times 1.6$ GeV for a small electric charge $q << 2\pi/e^2$. The hairy dyonic black hole with an integer charge, however is not stable and can decay into a magnetic one plus charged fermions. Their work also indicates that a hairy magnetic black hole can evolve via Hawking radiation into a nearly extremal one that is cosmologically stable. Our work of magnetic black hole in this paper has some differences as well as similarities with the magnetic black hole in Ref. [26], which will be discussed in Sect. 5.

2 Einstein–Weinberg–Salam theory

We consider the SU(2)× U(1) EWS action as

$$S = S_G + S_M = \int L_G \sqrt{-g}\, d^4x + \int L_M \sqrt{-g}\, d^4x, \quad (1)$$

with

$$L_G = \frac{R}{16\pi G}, \quad (2)$$

and

$$L_M = -\frac{1}{4} F^a_{\mu\nu} F^{a\mu\nu} - \frac{\epsilon\,(\phi)}{4} f_{\mu\nu} f^{\mu\nu} - \left(\hat{D}_\mu \phi\right)^\dagger \left(\hat{D}^\mu \phi\right) - \frac{\lambda}{2}\left(\phi^\dagger \phi - \frac{\mu^2}{\lambda}\right)^2, \quad (3)$$

where

$$\begin{aligned} F^a_{\mu\nu} &= \partial_\mu A^a_\nu - \partial_\nu A^a_\mu + g\epsilon^{abc} A^b_\mu A^c_\nu, \\ f_{\mu\nu} &= \partial_\mu B_\nu - \partial_\nu B_\mu, \\ \hat{D}_\mu \phi &= \left(\partial_\mu - \frac{ig}{2}\sigma^a A^a_\mu - \frac{ig'}{2} B_\mu\right)\phi, \end{aligned} \quad (4)$$

here ϕ is the Higgs doublet, $F^a_{\mu\nu}$ and $f_{\mu\nu}$ are the gauge field strengths of SU(2) and U(1) with potentials A^a_μ and B_μ, and g and g' are the corresponding coupling constants. Also $\hat{D}_\mu$ is the covariant derivative of the SU(2) × U(1) group.

The function $\epsilon\,(\phi)$ in Eq. (3) is a positive dimensionless function of the Higgs doublet which tends to unity asymptotically. In general, $\epsilon\,(\phi)$ modifies the permeability of the hypercharge U(1) gauge field while retaining the SU(2) x U(1) gauge symmetry. The term ϵ serves to regularize the point singularity that arises from the U(1) part. This is because ϵ effectively changes the $U(1)_Y$ gauge coupling g' to the 'running' coupling $\bar{g}' = g'/\sqrt{\epsilon}$, and by making $\bar{g}'$ infinite at the origin one can regularize the Cho–Maison monopole. For more details in the regularization, Refs. [14–17] are referred.

To construct globally regular gravitating monopole and magnetically charged black hole, we consider the spherically symmetric Schwarzschild-like metric

$$ds^2 = -N^2 A\, dt^2 + \frac{1}{A} dr^2 + r^2 d\theta^2 + r^2 \sin^2\theta\, d\varphi^2, \quad (5)$$

with

$$A = 1 - \frac{2Gm}{r}, \quad (6)$$

and the following electrically neutral ansatz for the matter functions,

$$\begin{aligned} &\phi = \frac{H}{\sqrt{2}}\,\xi, \quad \xi = i\begin{bmatrix} \sin\frac{\theta}{2}\, e^{-i\varphi} \\ -\cos\frac{\theta}{2} \end{bmatrix}, \\ &A^a_0 = 0, \quad A^a_i = -\frac{(1-K)}{gr}\hat{\varphi}^a\hat{\theta}_i + \frac{(1-K)}{gr}\hat{\theta}^a\hat{\varphi}_i, \\ &B_0 = 0, \quad B_i = -\frac{1}{g'}\frac{(1-\cos\theta)}{r\sin\theta}\hat{\varphi}_i, \end{aligned} \quad (7)$$

where N, A, m, K and H are all functions of r. In magnetic ansatz (7), the spatial spherical coordinate unit vectors are

$$\begin{aligned} \hat{r}_i &= \sin\theta\cos\varphi\,\delta_{i1} + \sin\theta\sin\varphi\,\delta_{i2} + \cos\theta\,\delta_{i3}, \\ \hat{\theta}_i &= \cos\theta\cos\varphi\,\delta_{i1} + \cos\theta\sin\varphi\,\delta_{i2} - \sin\theta\,\delta_{i3}, \\ \hat{\varphi}_i &= -\sin\varphi\,\delta_{i1} + \cos\varphi\,\delta_{i2}, \end{aligned} \quad (8)$$

whereas the isospin coordinate unit vectors with φ-winding number $n = 1, 2, 3, ...$ are

$$\begin{aligned}\hat{r}^a &= \sin\theta\cos n\varphi\,\delta_1^a + \sin\theta\sin n\varphi\,\delta_2^a + \cos\theta\,\delta_3^a,\\ \hat{\theta}^a &= \cos\theta\cos n\varphi\,\delta_1^a + \cos\theta\sin n\varphi\,\delta_2^a - \sin\theta\,\delta_3^a,\\ \hat{\varphi}^a &= -\sin n\varphi\,\delta_1^a + \cos n\varphi\,\delta_2^a.\end{aligned} \tag{9}$$

The value of n is set to one in this paper.

The tt and rr components of the Einstein equations then yield the equations for the metric functions

$$\frac{N'}{N} = 4\pi G r\left(\frac{2K'^2}{g^2r^2} + H'^2\right), \tag{10}$$

and

$$\begin{aligned}m' = 4\pi r^2\Bigg\{&A\left(\frac{K'^2}{g^2r^2} + \frac{H'^2}{2}\right) + \frac{\left(K^2-1\right)^2}{2g^2r^4}\\ &+ \frac{\lambda}{8}\left(H^2 - \frac{2\mu^2}{\lambda}\right)^2 + \frac{\epsilon}{2g'^2r^4} + \frac{1}{4}\frac{H^2K^2}{r^2}\Bigg\}.\end{aligned} \tag{11}$$

The equations for the matter functions read

$$AK'' + \left(A' + A\frac{N'}{N}\right)K' + \frac{\left(1-K^2\right)K}{r^2} - \frac{1}{4}g^2H^2K = 0, \tag{12}$$

and

$$\begin{aligned}&AH'' + \left(A' + \frac{2A}{r} + A\frac{N'}{N}\right)H' - \frac{HK^2}{2r^2}\\ &-\frac{\lambda}{2}\left(H^2 - \frac{2\mu^2}{\lambda}\right)H - \frac{1}{2g'^2r^4}\frac{d\epsilon\,(H)}{dH} = 0.\end{aligned} \tag{13}$$

Prime denotes derivative with respect to r, and $H_0 = \sqrt{2}\mu/\sqrt{\lambda}$ is the Higgs vacuum expectation value.

To facilitate numerical calculation, we consider the following dimensionless coordinate x and dimensionless mass function $\widetilde{m}$,

$$x = M_{\rm W}r, \quad \widetilde{m} = GM_{\rm W}m, \tag{14}$$

with $M_{\rm W} = \frac{1}{2}gH_0$. The Higgs field is also rescaled as $H \to H_0H$ and the solutions then depend on coupling constant α and β, where

$$\alpha^2 = 4\pi G H_0^2, \quad \beta^2 = \frac{\lambda}{g^2}, \tag{15}$$

as well as the Weinberg angle $\theta_{\rm W}$.

With Eqs. (14)–(15), the full set of Eqs. (10)–(13) transform into

$$\begin{aligned}&\frac{1}{N}\frac{dN}{dx} = \alpha^2x\left[\frac{1}{2x^2}\left(\frac{dK}{dx}\right)^2 + \left(\frac{dH}{dx}\right)^2\right],\\ &\frac{d\widetilde{m}}{dx} = \alpha^2x^2\left\{\frac{A}{2}\left[\frac{1}{2x^2}\left(\frac{dK}{dx}\right)^2 + \left(\frac{dH}{dx}\right)^2\right]\right.\\ &\qquad\left. + \frac{\left(K^2-1\right)^2}{8x^4} + \frac{\beta^2}{2}\left(H^2-1\right)^2 + \frac{\epsilon}{8\omega^2x^4} + \frac{H^2K^2}{4x^2}\right\},\\ &A\frac{d^2K}{dx^2} + \left(\frac{dA}{dx} + \frac{A}{N}\frac{dN}{dx}\right)\frac{dK}{dx}\\ &\qquad + \frac{\left(1-K^2\right)K}{x^2} - H^2K = 0,\\ &A\frac{d^2H}{dx^2} + \left(\frac{dA}{dx} + \frac{2A}{x} + \frac{A}{N}\frac{dN}{dx}\right)\frac{dH}{dx} - \frac{HK^2}{2x^2}\\ &\qquad -2\beta^2\left(H^2-1\right)H - \frac{1}{8\omega^2x^4}\frac{d\epsilon}{dH} = 0,\end{aligned} \tag{16}$$

where $\omega = g'/g = \tan\theta_{\rm W}$. Here we consider physical value of $\omega = 0.53574546$ by adopting $\sin^2\theta_{\rm W} = 0.22301323$ [27]. Since $M_{\rm H} = \sqrt{2}\mu$ and $M_{\rm W} = \frac{1}{2}gH_0$, we may also put Eq. (15) in the form of

$$\alpha = \sqrt{4\pi G}H_0 = \sqrt{4\pi}\frac{H_0}{M_{\rm p}}, \quad \beta = \frac{1}{2}\frac{M_{\rm H}}{M_{\rm W}}, \tag{17}$$

where by adopting physical values of $M_{\rm H} = 125.10$ GeV and $M_{\rm W} = 80.379$ GeV, the physical value of β used here is 0.77818833.

Notice that the first equation of Eq. (16) depends explicitly on K and H. Hence substituting the first equation of Eq. (16) into the third and fourth equation of Eq. (16), we need to solve only three equations for K, H and A. Obviously solutions to Eq. (16) depend on the permeability function ϵ. In the paper by Cho et al. [25], the form of $\epsilon = (H/H_0)^8$ is considered. In a recent paper [17], $\epsilon = (H/H_0)^p$ is also possible. For the sake of simplicity, we considered $p = 8$ in this paper. However we would like to point out that all values of $p = 1, 2, 3, ...8$ seem to produce convergent numerical results.

As our solution is electrically neutral, following Ref. [28], we consider a special solutions of Eq. (16), which is the embedded RN solutions with mass $\widetilde{m}_\infty$ and magnetic charge near unity,

$$\begin{aligned}&\widetilde{m}(x) = \widetilde{m}_\infty - \frac{\alpha^2}{8x}\left(1 + \frac{\epsilon}{\omega^2}\right), \quad N(x) = 1,\\ &K(x) = 0, \quad H(x) = 1,\end{aligned} \tag{18}$$

where we will consider $\epsilon = 1$ as $H = 1$. The corresponding extremal RN solutions then possess horizon $x_{\rm H}$, where

$$x_{\rm H} = \widetilde{m}_\infty = \frac{\alpha}{2}\sqrt{1 + \frac{1}{\omega^2}}. \tag{19}$$

From Eqs. (14) and (18), the ADM mass can be defined as

$$m_{\rm ADM} = \frac{4\pi H_0^2}{M_{\rm W}}\frac{\widetilde{m}_\infty}{\alpha^2}, \tag{20}$$

where one can readily read off the value for ADM mass from the plot of $\widetilde{m}_\infty/\alpha^2$ versus α.

3 Gravitating monopole

We first consider globally regular gravitating monopole solutions. Asymptotic flatness requires that the metric functions N and A both approach a constant at spatial infinity. We here adopt

$$N(\infty) = 1, \quad \widetilde{m}(\infty) = \widetilde{m}_\infty. \tag{21}$$

This means that $\widetilde{m}(\infty)$ which determines the total mass of the monopole is not constrained. The matter functions also approach constant asymptotically as

$$K(\infty) = 0, \quad H(\infty) = 1. \tag{22}$$

On the other hand, regularity at the origin requires

$$K(0) = 1, \quad H(0) = 0, \quad \widetilde{m}(0) = 0. \tag{23}$$

In SU(2) EYMH theory [9,10], the gravitating monopole solution emerges smoothly from the flat space 't Hooft–Polyakov monopole ($\alpha = 0$) before becoming a limiting solution at some critical value of gravitational coupling α_c and ceases to exist beyond α_c. One generally expects that α_c should be the maximal value of gravitational coupling, α_{max}. However, results shows that α_{max} does not correspond to the zero of the metric function (in their notation μ) when $\beta = 0$. The tabulated value is $\alpha_{max} = 1.403$ corresponds to $\mu_{min} = 0.03$. From α_{max} instead the branch of solution bends backward, up to the critical coupling constant α_c before the zero for μ_{min} is formed and the solution becomes limiting solution (when $\alpha_c = 1.386$, $\mu_{min} = 8.07 \times 10^{-9}$). In general, the (normalized) mass of gravitating monopole solution decreases with increasing gravitational coupling until the maximal gravitational coupling $\alpha_{max} = 1.403$.

Our results in EWS theory are plotted in Fig. 1. The metric function $A(x)$ starts to develop a pronounced minimal value (A_{min}) with increasing α from $\alpha = 0$ up to a maximal value α_{max}, indicating that gravitating Cho–Maison monopole emerges smoothly from the flat space Cho–Maison monopole. The value of A_{min} decreases from one to zero at α_{max} where the branch of solution becomes a black hole and ceases to exist. In our solutions, α_{max} always corresponds to the lowest value of A_{min} ($\alpha_{max} = 1.814$ for $A_{min} = 3.2992 \times 10^{-6}$). In other words, $\alpha_{max} = \alpha_c$ in EWS theory. We have tried to search for possible lower value of A_{min} by considering the coupling constant α bending backwards but the results for A_{min} is always higher than the lowest A_{min} at $\alpha_{max} = 1.814$. These results are tabulated in Table 1 (the numerical method used in this paper is different to that of [9,10]).

Of course the existence of $\alpha_{max} > \alpha_c$ in EYMH theory has been observed for β up to 0.7 [9,10]. It is most profound when $\beta = 0$, where $\alpha_{max} = 1.403$ (for $\mu_{min} = 0.035$) and $\alpha_c = 1.386$ (for $\mu_{min} = 8.07 \times 10^{-9}$). When $\beta = 0.7$, $\alpha_{max} = 1.26027253$ (for $\mu_{min} = 0.035$) and $\alpha_c = 1.2602718$ (for $\mu_{min} = 8.07 \times 10^{-9}$). In this case, if large β is considered in EYMH theory, one should get $\alpha_{max} \approx \alpha_c$. This has been further confirmed in Refs. [29,30]. Then question arises if the non-existence of $\alpha_{max} > \alpha_c$ in EWS theory might due to higher value of β considered ($\beta = 0.77818833$).

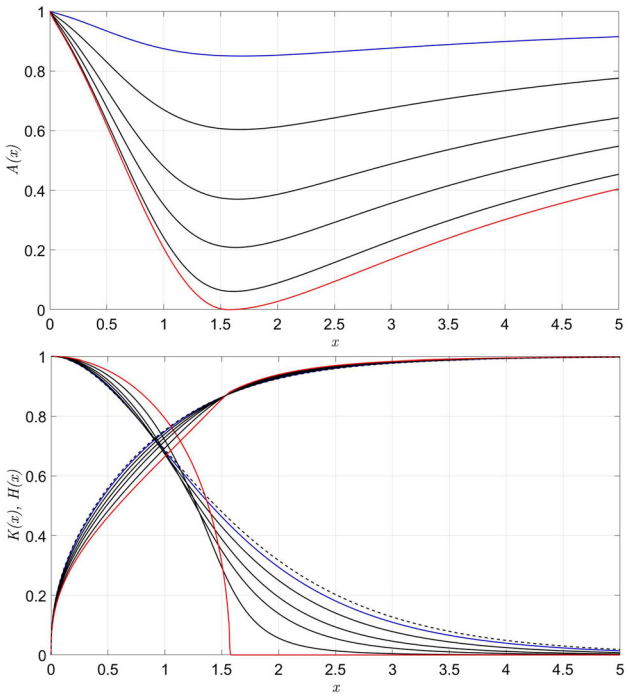

Fig. 1 Functions of $A(x)$, $K(x)$ and $H(x)$ versus x of the fundamental gravitating electroweak monopole with physical β and Weinberg angle for $\alpha = 0.6$ (blue), 1.0, 1.3, 1.5, 1.7 and 1.814 (red). Dashed line indicates non-gravitating monopole

Table 1 Table of A_{min} for selected values of α near α_{max} for radial excitation (r.e.) and gravitating monopole (g.m.)

α	A_{min}(r.e.)	A_{min}(g.m.)
1.53	2.5783×10^{-4}	0.1849
1.54	1.8504×10^{-4}	0.1771
1.55	1.2296×10^{-4}	0.1694
1.56	7.2356×10^{-5}	0.1617
1.57	1.2173×10^{-5}	0.1540
1.58	6.7480×10^{-6}	0.1464
1.584	5.4718×10^{-6}	0.1434
1.76	–	0.0243
1.77	–	0.0188
1.78	–	0.0137
1.79	–	0.0089
1.80	–	0.0045
1.81	–	8.2190×10^{-4}
1.814	–	3.2992×10^{-6}

For the above reason, we first compute the gravitating monopole solutions when $\beta = 0.77818833$ in EYMH theory. Our numerical results shows that even for $\beta = 0.77818833$, the solutions possess phenomena of $\alpha_{\max} > \alpha_{\rm c}$, where $\alpha_{\max} = 1.2203$ for $A_{\min} = 1.6388 \times 10^{-5}$ and $\alpha_{\rm c} = 1.2123$ for $A_{\min} = 1.2211 \times 10^{-5}$. For the sake of comparison, we also compute gravitating Cho–Maison monopole solution when $\beta \to 0$. Results again show that in EWS theory $\alpha_{\max}$ always correspond to lowest value of the metric function $A(x)$. This confirms that the non-existence of $\alpha_{\max} > \alpha_{\rm c}$ is a generic feature of EWS theory. However we are not interested for $\beta \to 0$ in EWS theory since it is not physical.

In general, our results of gravitating Cho–Maison monopole are quite identical to the gravitating 't Hooft–Polyakov monopole in SU(2) EYMH theory except for the non-existence of 'backward bending' in α (or $\alpha_{\max} > \alpha_{\rm c}$). Hence our results can be viewed as having distinctive characteristics compared to that in EYMH theory, though both approach their respective limiting solutions at some specific value of gravitational coupling. Moreover, contrary to gravitating monopole in EYMH theory, results in EWS theory describes a genuine gravitating Cho–Maison monopole turning into a black hole.

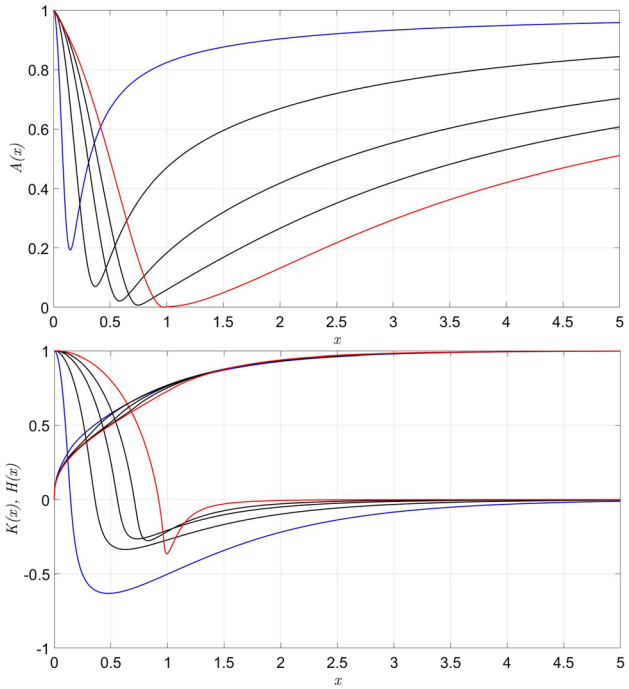

Fig. 2 Functions of $A(x)$, $K(x)$ and $H(x)$ versus x of the radial excitation for $\alpha = 0.2$ (blue), 0.6, 1.0, 1.25 and 1.5 (red), for physical β and Weinberg angle

4 Radially excited monopole

For EYMH theory, besides the branch of fundamental gravitating monopole solution, there exist branches of radially excited monopole solutions. While the gauge field function of the fundamental monopole solution decreases monotonically to zero, this is not the case for radially excited solutions. In general, gauge field function of the n-th excited monopole solutions develop n minimum node before tending to zero at spatial infinity. Similar to fundamental monopole solution, radially excited monopole solutions also exist below some maximal value of the gravitational constant α. However, they have no flat space counterpart as $\alpha \to 0$, but tends to the Bartnik–Mckinnon solution of EYM theory .

In EWS theory, we also observed similar radially excited monopole solution, as shown in Fig. 2. The gauge field function $K(x)$ of the (1st) radially excited solution does not decrease monotonically to zero, it develops a minimum node before approaches zero at spatial infinity. These radial excitations only exist below some maximal value of the gravitational constant, $\alpha_{\max} = 1.584$. They similarly do not have flat space counterpart as $\alpha \to 0$. Following the gravitating monopole in previous section, we also tabulate the value of $A_{\min}$ for values of α near $\alpha_{\max}$ in Table 1. We again observed no 'backward-bending' of the solution branch as reported in Refs. [9,10].

Following Ref. [28], we plot the normalized mass $\widetilde{m}_\infty/\alpha^2$ versus α for radial excitation in Fig. 3 (included in the same graph is the corresponding plot for fundamental gravitating monopole). As expected, the radial excitation branch possesses higher normalized mass than that of the fundamental gravitating monopole. In the limit of $\alpha \to 0$, the normalized mass of the fundamental gravitating monopole converges to a finite value (0.7197), whereas that of radial excitation diverges to infinity. This coincides with the statement that radial excitation does not have flat space counterpart. Both massess of the fundamental monopole and radial excitation decrease with α, but mass of the gravitating monopole decreases monotonically while there is an inverse α fall-off for radial excitation.

At $\alpha_{\max}$, the radial excitation (as well as the fundamental monopole solutions) reaches their limiting functions but do not bifurcate with the branch of extremal RN solution. This is different from the results reported in Ref. [28], where at $\alpha_{\max}$ the fundamental monopole approaches its limiting solution and bifurcate with the branch of extremal RN solution (bottom plot of Fig. 3). The non-bifurcation originates from Eq. (18). Recall that in EYMH theory, the metric function of the embedded RN solution with magnetic charge P reads

$$A = 1 - \frac{2\widetilde{m}_\infty}{x} + \frac{\alpha^2}{x^2} P^2. \tag{24}$$

Eq. (18) gives metric function of the embedded RN solution of EWS theory as

$$A = 1 - \frac{2\widetilde{m}_\infty}{x} + \frac{\alpha^2}{x^2}\frac{1}{4}\left(1 + \frac{\epsilon}{\omega^2}\right). \tag{25}$$

From Eq. (25), evaluating the third term by considering $\epsilon = 1$ and $\omega = 0.53574546$, we find that the magnetic charge of embedded RN solution is 1.0588, which is slightly higher than one and this contributes to the non-bifurcation (note that the gravitating monopole or radially excited monopole has unit magnetic charge).

Hence in general our results of radially excited Cho–Maison monopole are quite identical to the radially excited monopole in SU(2) EYMH theory. There are of course some key differences. First, radial excitation (as well as gravitating monopole) does not bifurcate with the branch of extremal RN solution at $\alpha_{\max}$. We expect that a different (more realistic) form of ϵ will contribute to the bifurcation, but that remains to be answered in future investigation. Second, for a given α, the mass of radial excitation (or gravitating monopole) in EWS theory is always lower than the mass of their counterpart in EYMH theory. This is evident from Fig. 3.

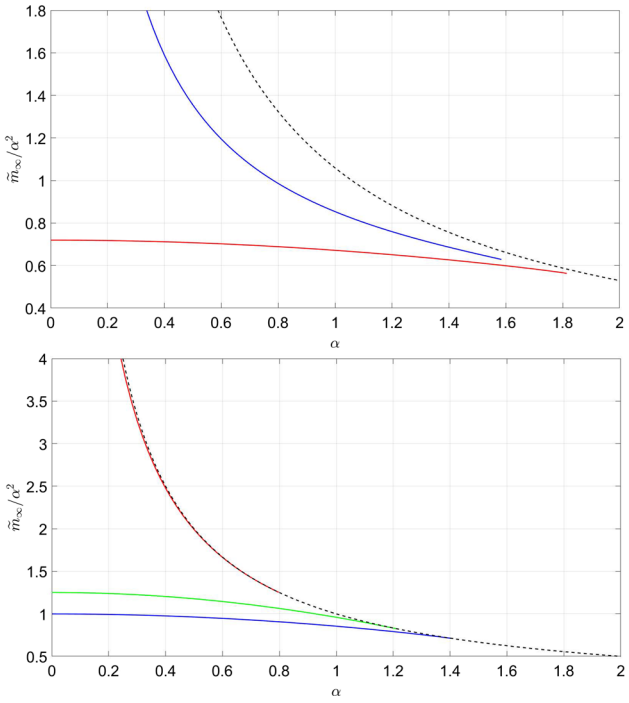

Fig. 3 Top: Plot of $\widetilde{m}_\infty/\alpha^2$ versus α for gravitating monopole (red), radial excitation (blue) and the extremal RN solution (dashed line) of the EWS theory. Bottom: Plot of $\widetilde{m}_\infty/\alpha^2$ versus α for gravitating monopole (blue), radial excitation (red) and the extremal RN solution (dashed line) of the EYMH theory when $\beta = 0$. Green line represents the gravitating monopole when $\beta = 0.77818833$

5 Black hole solutions

In SU(2) EMYH theory, there exist special kind of non-Abelian black hole solutions which is different from the embedded RN black hole solutions. These black hole solutions emerge from the globally regular monopole solution when a finite regular event horizon is imposed. Characterized as 'black hole within magnetic monopole', these solutions provide counter-examples to the 'no hair' conjecture. With increasing horizon radius $x_{\rm H}$, depending on the value of gravitational coupling α, these non-Abelian black hole either merges with Abelian RN black hole at some critical horizon radius (for $0 < \alpha < \frac{1}{2}\sqrt{3}$), or ceases to exist at some maximal value of $x_{\rm H}$ when a second zero of the metric function is formed (for $\frac{1}{2}\sqrt{3} < \alpha < \alpha_{\max}$, where $\alpha_{\max} = 1.403$). These behaviours of SU(2) EYMH black hole solutions are shown in Fig. 4.

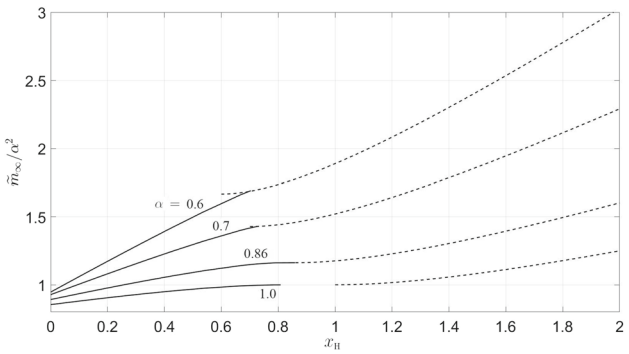

Fig. 4 The (normalized) mass of the EYMH black hole solutions $\widetilde{m}_\infty/\alpha^2$ as a function of horizon radius $x_{\rm H}$ for $\alpha = 0.6, 0.7, 0.86$ and 1.0, together with the corresponding RN solutions with unit magnetic charge (dashed lines)

We now consider such non-Abelian black hole solutions in EWS theory. Consider again asymptotic flatness, they satisfy the same boundary conditions at spatial infinity as the globally regular solutions, Eqs. (21) and (22). The existence of a regular event horizon requires

$$\widetilde{m}\,(x_{\rm H}) = \frac{x_{\rm H}}{2}, \quad N\,(x_{\rm H}) < \infty. \tag{26}$$

The matter functions must also satisfy

$$\left.\frac{dA}{dx}\frac{dK}{dx}\right|_{x_{\rm H}} = K\left(H^2 - \frac{1-K^2}{x^2}\right)\Big|_{x_{\rm H}}, \tag{27}$$

and

$$\left.\frac{dA}{dx}\frac{dH}{dx}\right|_{x_{\rm H}} = H\left(\frac{K^2}{2x^2} + 2\beta^2\left(H^2-1\right) + \frac{1}{2\omega^2 x^4 H}\frac{d\epsilon}{dH}\right)\Big|_{x_{\rm H}}. \tag{28}$$

In particular, for a given coupling constant α, black hole solutions corresponding to the fundamental mono-pole

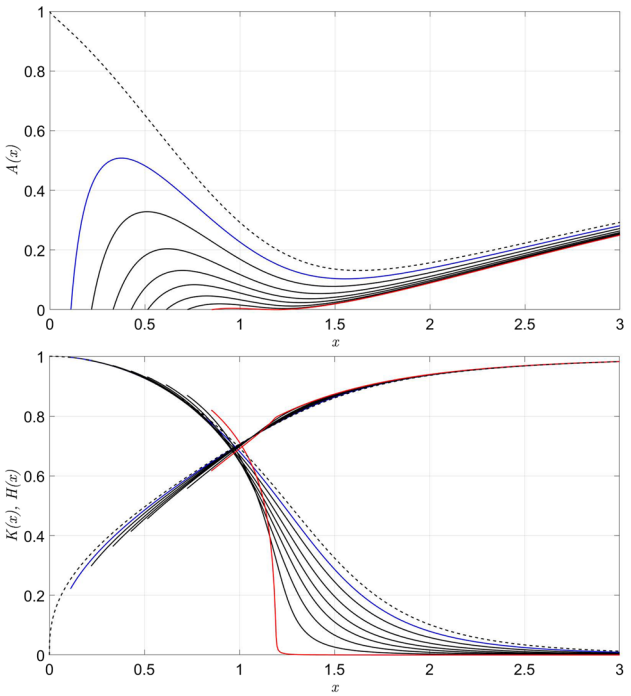

Fig. 5 Black hole in electroweak monopole solutions with $\alpha = 1.6$, physical β and Weinberg angle, plotted as a function of x for $x_{\rm H} = 0.1111$ (blue), 0.2195, 0.3333, 0.4286, 0.5152, 0.6129, 0.7241 and 0.8519 (red). Dashed lines indicate regular gravitating solutions

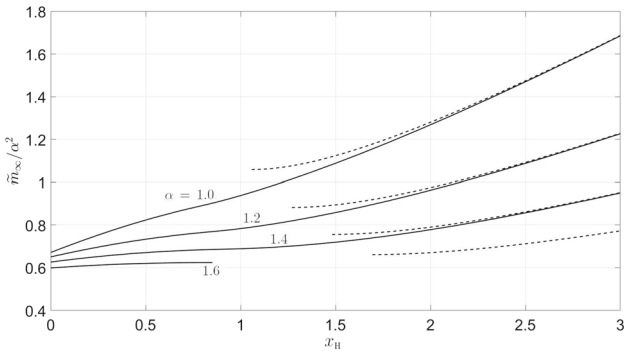

Fig. 6 The (normalized) mass of the EWS black hole solutions $\widetilde{m}_\infty/\alpha^2$ as a function of the horizon radius $x_{\rm H}$ for the values of coupling constant $\alpha = 1.0$, 1.2, 1.4 and 1.6, together with the corresponding RN solutions with unit magnetic charge (dashed lines)

branch emerge from globally regular solution in the limit $x_{\rm H} \to 0$ and persist up with increasing horizon radius. We first consider the case of relatively large α ($\alpha = 1.6$). With increasing horizon radius, limiting solution is reached at a maximal value of horizon radius ($x_{\rm H} = 0.8519$), where a second zero of $A(x)$ is formed, Fig. 5. For smaller values of α, black hole solutions do not reach limiting solutions but merge with the corresponding non-extremal RN solutions. This behaviour which is reminiscent of SU(2) EYMH theory can be understood clearer from Fig. 6, which shows the black hole solutions emerge from globally regular monopole solutions in the limit of $x_{\rm H} \to 0$ and persist up with increasing $x_{\rm H}$. For $0 < \alpha < 1.576$, the black hole solutions slowly converge to the corresponding non-extremal RN solutions at large horizon radius. For $1.576 < \alpha < \alpha_{\rm max}$ where $\alpha_{\rm max} = 1.814$, they however become limiting solution at maximal value of horizon radius.

To better illustrate the solutions, following Refs. [9,10], we also present the 'phase diagram' of black hole solution in EWS theory for physical β and Weinberg angle in Fig. 7. Non-Abelian black hole exist in regions of the $(\alpha, x_{\rm H})$ plane denoted by I and II. RN black holes as given by Eq. (18), exist in regions II and III, whereas in region IV there are no non-Abelian black hole solutions. The boundary $x_{\rm H} = 0$ of region I corresponds to the regular gravitating solutions. The cut-off point of $\alpha = 1.576$ as mentioned above is seen as separating region I into Ia and Ib. Approaching the curve AB in region Ia, the solutions develop double zero in $A(x)$ and they become limiting solutions. In region Ib, the non-Abelian solutions extend into region II and slowly merge into the RN solution with increasing $x_{\rm H}$.

Hence the 'black hole in Cho–Maison monopole' of EWS theory again have identical features as the 'black hole in monopole' of SU(2) EYMH theory [9,10,28]. There are however some key differences:

1. First (for small α) the EWS black hole solutions do not merge with the corresponding RN solution at critical horizon radius, but only converges towards them slowly with increasing horizon radius. The EYMH black hole solutions merge with the non-extremal RN solutions at critical value of the horizon radius [28].
2. Second, for region of $(\alpha, x_{\rm H})$ plane where non-Abelian black hole and RN black holes coexist, the mass of non-Abelian black hole solution is always lower than the mass of RN solution ($m_{\rm n.a.}/m_{\rm RN} \leq 1$). The case in EYMH theory is however more complicated. The region of coexistence for non-Abelian black hole and RN solution exists for $0 < \alpha < 0.77$. Here the mass of non-Abelian black hole is smaller than the mass of RN solution ($m_{\rm n.a.}/m_{\rm RN} < 1$), but there also exists small region where $m_{\rm n.a.}/m_{\rm RN} > 1$. Then for $0.77 < \alpha < 0.866$, non-Abelian black hole solution joints smoothly with the RN solution at critical value of horizon radius. For $0.866 < \alpha < 1.403$, non-Abelian black hole solution reach limiting solution at maximal value of horizon radius, and does not bifurcate with the RN solution.
3. Third, for a given horizon radius $x_{\rm H}$, the mass of black hole in EWS theory always has a lower value than its counterpart in EYMH theory.

As mentioned in Sect. 1, there is also report on hairy magnetic and dyonic black holes in the Standard Model and gen-

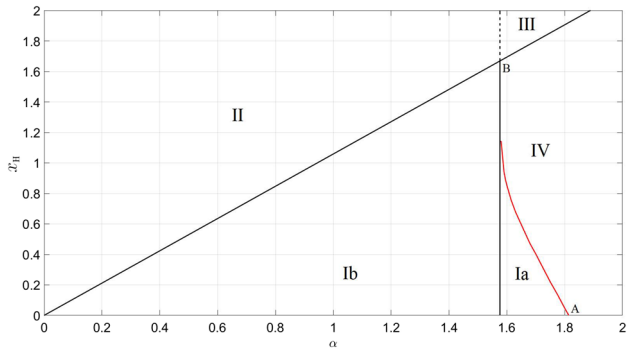

Fig. 7 'Phase diagram' of black hole solution in Einstein–Weinberg–Salam theory for physical β and Weinberg angle

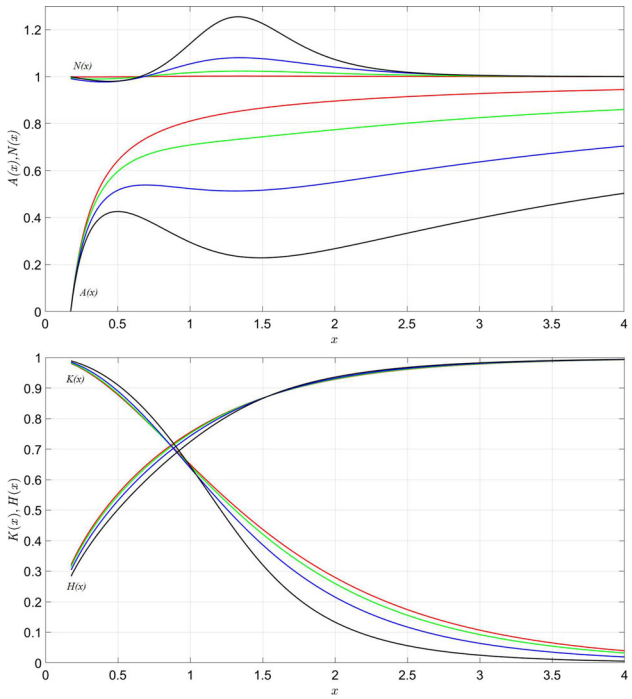

Fig. 8 Plot of function $A(x)$, $N(x)$ versus x (top) and $K(x)$, $H(x)$ versus x (bottom) of the EWS magnetically charged black hole for $\alpha = 0.2$ (red), 0.6 (green), 1.0 (blue) and 1.4 (black) at fixed horizon radius $x_H = 0.1765$

eral relativity [26]. Our work of magnetic black hole here share some differences and similarities with the magnetic black hole in Ref. [26]. First, our Lagrangian (3) contains a positive dimensionless modification term $\epsilon(\phi)$ that modifies the permeability of the hypercharge U(1) field but still retains SU(2) $\times$ U(1) symmetry of the effective Lagrangian. The Lagrangian in Ref. [26] is without this modification term. Both our results and that of Ref. [26] shows a magnetically charged black hole that possesses 'hairy' cloud of electroweak gauge and Higgs function outside the event horizon. However it seems there is a difference in the behaviour of the metric functions. Referring to Fig. 5, our metric function A increases from zero at the horizon radius, then develops a local maximum and minimum before tending to unity asymptotically. The corresponding metric function A in Ref. [26] (denoted as N in the paper) increases monotonically from zero at the horizon radius to unity asymptotically.

To further investigate, we plot the functions of K, H, A and N for selected values of $\alpha = 0.2, 0.6, 1.0$ and 1.4 at a fixed horizon radius $x_H = 0.1765$ in Fig. 8. When α is relatively large, the function A has a more pronounced local minimum and local maximum before approaches one asymptotically. When α becomes smaller, A becomes a monotonic increasing function from $A = 0$ at the horizon radius to $A = 1$ at spatial infinity. The function N also generally shows a minimum and maximum outside the event horizon before approaching unity asymptotically. As α becomes smaller, so are the maximum/minimum and function N becomes approximately one at small $\alpha = 0.2$. This coincides with the fact that the corresponding metric function N in Ref. [26] (denoted as P) is mentioned to have value of approximately one. This confirms that the magnetic black hole in Ref. [26] is analogous to the specific case of small α of our general spectrum of magnetic black hole solutions. Referring to the 'phase diagram' of magnetically charged black hole as in Fig. 7, the results of Ref. [26] is located in region Ib (southwest corner of the plot).

There are also some concerns that the black hole will evolve via the emission of Hawking radiation, leading to the evaporation of black hole and exposing the singularity. However, again take note that our Lagrangian in Eq. (3) has a modification term $\epsilon(\phi)$ that serves to regularize the singularity originating from the U(1) part, so that the magnetic monopole here is a regularized finite energy object rather than a singular one. Even for the case of pure gravitationally coupled Weinberg Salam model without the modification term [26], result shows that a hairy black hole will evolve into an (nearly) extremal RN black hole via emission of Hawking radiation. We believe that our magnetic black hole will follow similar path as in Ref. [26]. The details will be reported in a future work.

6 Conclusions

We have studied numerical solutions of the Einstein–Weinberg–Salam theory corresponding to: (1) fundamental gravitating electroweak monopole; (2) radially excited electroweak monopole; and (3) non-Abelian magnetically charged black hole.

The fundamental monopole solution emerges from the corresponding flat space monopole solution and extends smoothly up to a maximal value of the gravitational coupling

Table 2 The numerical estimate of ADM mass for gravitating monopole (g.m.) and radial excitation (r.e.) with $\epsilon = (H/H_0)^8$ and physical value of β

α	ADM mass (r.e.)	ADM mass (g.m.)
0	∞	6.821 TeV
0.20	25.555 TeV	6.802 TeV
0.40	15.058 TeV	6.747 TeV
0.60	11.320 TeV	6.656 TeV
0.80	9.344 TeV	6.529 TeV
1.00	8.089 TeV	6.367 TeV
1.20	7.198 TeV	6.171 TeV
1.40	6.506 TeV	5.942 TeV
1.584	Black hole	5.702 TeV
1.80	–	5.369 TeV
1.814	–	Black hole

constant $\alpha_{\max}$, before they collapse into a black hole. Besides the fundamental monopole branch, there exist branches of radially excited monopole solution, which also exist up to a maximal value of α. However there are no flat space counterpart in the limit of $\alpha \to 0$ for the radially excited solution.

Both the normalized mass of fundamental monopole and radial excitation decrease with α, with radial excitation branch possesses higher mass than that of the fundamental gravitating monopole. In the limit of $\alpha \to 0$, the normalized mass of the fundamental monopole branch converges to a finite value (0.7197), indicating the ADM mass of approximately 6.821 TeV. On the other hand the normalized mass of radial excitation diverges to infinity as $\alpha \to 0$, indicating that the radial excitation does not have flat space counterpart. We summarize the numerical estimate of ADM mass for gravitating monopole and radial excitation for selected values of α in Table 2.

For the 'black hole in electroweak monopole', black hole solutions corresponding to fundamental monopole branch emerge from globally regular solution in the limit $x_{\rm H} \to 0$ and persist up differently (depending on coupling constant α) with increasing horizon radius. For a relatively large α ($1.576 < \alpha < 1.814$), limiting solution is reached at a maximal value of horizon radius, e.g. $x_{\rm H}(\max) = 0.8519$ for $\alpha = 1.6$. However for smaller values of α ($0 < \alpha < 1.576$), black hole solutions do not reach limiting solutions but slowly merge into the corresponding non-extremal RN solutions at large horizon radius.

Despite mostly identical, our results in Einstein–Weinberg–Salam theory have some key differences compared to that of EYMH theory: (1) Our solutions of gravitating monopole and radial excitation do not exhibit the phenomena of 'backward-bending' in coupling constant α as observed in Refs. [9,10,28]. The maximal value $\alpha_{\max}$ always correspond to the lowest value of the metric function A and the solutions become limiting solutions at $\alpha_{\max}$. (2) At $\alpha_{\max}$, both the (normalized) mass of gravitating monopole and radial excitation reaches minimum value but do not bifurcate with the branch of extremal RN solution respectively. (3) The non-Abelian black hole solution converges slowly into the corresponding non-extremal RN solutions with large horizon radius. At a given horizon radius where the non-Abelian black hole and RN solution coexist, the mass of non-Abelian black hole is always lower than the mass of RN solution. (4) At a given α, the mass of gravitating monopole (or radial excitation) in EWS theory always has lower value than its counterpart in EYMH theory. Similarly, at a given horizon radius $x_{\rm H}$, the mass of black hole in EWS theory is also lower than the mass of its counterpart in EYMH theory. This suggests that the configurations in EWS theory are more stable.

In SU(2) EYMH theory, gravitating monopoles and magnetically charged black holes can be generalized to gravitating dyons and dyonic black holes [28]. Hence our results here clearly have the dyonic generalization simply by switching on the time component of the gauge potential. We will discuss these findings in a separate paper.

Data Availability Statement This manuscript has no associated data or the data will not be deposited. [Authors' comment: Protection of participant and intellectual property.]

Funded by SCOAP[3].

References

1. P.A.M. Dirac, Proc. R. Soc. Lond. A **133**, 60 (1931)
2. P.A.M. Dirac, Phys. Rev. **74**, 817 (1948)
3. T.T. Wu, C.N. Yang, in *Properties of Matter under Unusual Conditions*, ed. by H. Mark, S. Fernbach (Intersience, New York, 1969), p. 349
4. T.T. Wu, C.N. Yang, Nucl. Phys. B **107**, 365 (1976)
5. T.T. Wu, C.N. Yang, Phys. Rev. D **16**, 1018 (1977)
6. G. 't Hooft, Nucl. Phys. B **79**, 276 (1974)
7. A.M. Polyakov, JETP Lett. **20**, 194 (1974)
8. M.K. Prasad, C.M. Sommerfield, Phys. Rev. Lett. **35**, 760 (1975)
9. P. Breitenlohner, P. Forgacs, D. Maison, Nucl. Phys. B **383**, 357 (1992)
10. K. Lee, V.P. Nair, E.J. Weinberg, Phys. Rev. D **45**, 2751 (1992)
11. R. Bartnik, J. McKinnon, Phys. Rev. Lett. **61**, 141 (1988)
12. Y.M. Cho, D. Maison, Phys. Lett. B **391**, 360 (1997)

13. W.S. Bae, Y.M. Cho, J. Korean Phys. Soc. **46**, 791 (2005)
14. K. Kimm, J.H. Yoon, Y.M. Cho, Eur. Phys. J. C **75**, 67 (2015)
15. K. Kimm, J.H. Yoon, S.H. Oh, Y.M. Cho, Mod. Phys. Lett. A **31**, 1650053 (2016)
16. J. Ellis, N.E. Mavromatos, T. You, Phys. Lett. B **756**, 29 (2016)
17. P. Zhang, L. Zou, Y.M. Cho, Eur. Phys. J. C **80**, 280 (2020)
18. B. Acharya et al., (MoEDAL Collaboration), Phys. Rev. Lett. **118**, 061801 (2017)
19. B. Acharya et al., (MoEDAL Collaboration), Phys. Rev. Lett. **123**, 021802 (2019)
20. ATLAS Collaboration, Phys. Rev. Lett. **109**, 261803 (2012)
21. ATLAS Collaboration, Eur. Phys. J. C **75**, 362 (2015)
22. ATLAS Collaboration, Phys. Rev. Lett. **124**, 031802 (2020)
23. R. Abbasi et al., (IceCube Collaboration), Phys. Rev. D **87**, 022001 (2013)
24. M. Ahlers, K. Helbing, C. Heros, Eur. Phys. J. C **78**, 924 (2018)
25. Y.M. Cho, K. Kimm, J.H. Yoon, Phys. Lett. B **761**, 203 (2016)
26. Y. Bai, M. Korwar, J. High Energy Phys. **2021**, 119 (2021)
27. P.A. Zyla et al. (Particle Data Group), Prog. Theor. Exp. Phys. **2020**, 083C01 (2020)
28. Y. Brihaye, B. Hartmann, J. Kunz, Phys. Lett. B **441**, 77 (1998)
29. A. Lue, E.J. Weinberg, Phys. Rev. D **60**, 084025 (1999)
30. Y. Brihaye, B. Hartmann, J. Kunz, Phys. Rev. D **62**, 044008 (2000)